Journal of Mining and Earth Sciences

Website: http://tapchi.humg.edu.vn

Development of a new analytical model for the network-type tunnel ventilation systems

Hyo-Gyu Kim [1, *], Ji-Oh Ryu [2], Duc Van Nguyen [3], Chang-Woo Lee[4], Thao Qui Le[5]

[1] *Jusung G & B Inc., Seoul, Korea*
[2] *Dept. of Automotive Engineering, Shin-Han University, Uijeongbu, Korea*
[3] *Energy and Mineral Resources Engineering Departement, Dong-A University, Busan, Korea*
[4] *Energy and Mineral Resources Engineering Departement, Dong-A University, Busan, Korea*
[5] *Mining Engineering Departement, Universiy of Mining and Geology, Hanoi, Vietnam*

ARTICLE INFO

Article history:
Received 12 Sept. 2017
Accepted 15 Nov. 2017
Available online 29 Dec 2017

Keywords:
Tunnel ventilation
Hardy-Cross
Ventilation efficiency

ABSTRACT

Recently, various shapes of the ventilation split have been designed for urban underground vehicle tunnels at home and abroad. This requires a special analytical method different from the case of single-tube tunnels. However, since there is no design standard suggested for the analysis of network-type tunnel ventilation system, the various methods and tools have been widely applied. This study aims at deriving an analytical model appropriate for the network-type tunnel ventilation design. Hardy-Cross iteration method among the existing analytical techniques for network-type tunnel ventilation systems is relatively straightforward to understand and accordingly has been widely applied to the mine as well as tunnel ventilation systems. However, several limitations have been reported such as truncation errors associated with Taylor series expansion and convergence errors due to the mesh selection algorithm for the large-scale network-type tunnels. In this study, a new model to analyze the network-type tunnel ventilation system without mesh selection required for the Hardy-Cross iteration method is developed and its applicability is evaluated. The ultimate goal is to suggest an analytical method easy to apply for the network-type tunnel ventilation systems.

1. Introduction

Recently most of the urban tunnels at home and abroad tend to be longer and more complicated with slip tunnel connections, compared with the simple tube tunnels with one entrance and one exit portal. Furthermore, their cross-section becomes smaller and they go deeper. Some of them are constructed as network-type tunnels with multiple slip tunnels, rampways and ventilation shafts. Construction of network-type tunnels with slip tunnels is expected to increase mainly due to solve the urban traffic problems and utilize surface green zone more efficiently. Widely-known network-

*Corresponding author
E-mail: cwlee@dau.ac.kr

type tunnels are A86 in Paris, France, M30 in Madrid, Spain, Shinjuku Line and Shinagawa Line of the central ring road in Tokyo, Japan, underground roads (SR99 Project) in Seattle, U.S., Sodra Ranken Tunnel E4 Bypass Road in Stockholm, Sweden, Glen Johnson (CLEM7) Tunnel in Australia. In case of South Korea, Seoul U-Samrtway Plan, Jemulpo Tunnel, and Dongbu Expressway Underground Road tunnel are either planned or underway (Choi, 2016). Therefore, to optimize the ventilation system in network-type tunnels, there has been a need for providing design criteria suitable for network-type tunnel. As a result, a special analytical method different from the case of single-tube tunnels has been required. However, since there is no design method suggested for the analysis of network-type tunnel ventilation system, the existing methods for the network analysis have been widely applied.

Hardy-Cross iteration method among the existing network analytical techniques for network-type tunnel ventilation systems is relatively straightforward to understand and accordingly has been widely applied to the mine as well as tunnel ventilation systems. However, several limitations have been reported such as truncation error associated with Taylor series expansion and excessive convergence error due to the mesh selection algorithm for the large-scale network-type tunnels. In this study, a new model to analyze the network-type tunnel ventilation system without mesh selection compulsory for the Hardy-Cross iteration method is developed and its applicability is evaluated.

2. Forces acting in the tunnel ventilation system and network theory

If action ventilation in tunnels is expressed by the head concept of the length (m) unit, the forces acting in the tunnel ventilation system with jet fans include ventilation resistance force (ΔP_r), natural ventilation force (ΔP_m), traffic-induced force (piston effect) (ΔP_t) and jet fan ventilation force (ΔP_{jf}); these forces are defined as in Equations (1) to (4).

$$\Delta P_r(\mathrm{m}) = \frac{a}{A_r^2}.Q^2;\ a = \left(1 + \xi + \lambda\frac{L}{D}\right)\frac{1}{2g} \quad (1)$$

$$\Delta P_m(\mathrm{m}) = aV_n^2 \quad (2)$$

$$\Delta P_t(m) = bV_t^2 - \frac{2bV_t}{A_r}.Q + \frac{b}{A_r^2}.Q^2;\ b = \frac{A_m}{A_r}n_t \quad (3)$$

$$\Delta P_{jf}(m) = cV_j - \frac{c}{A_r}.Q;\ c = n_{jf}.K_j\frac{A_j}{A_r}\frac{1}{g}V_j \quad (4)$$

Where, a, b and c are constants, Q is airflow rate (m^3/s), A_r is cross-sectional area (m^2), V_n is air velocity induced by the negative natural ventilation force (m/s), V_t is vehicle speed (m/s), V_j is jet fan discharge velocity (m/s), ξ is entrance shock loss coefficient, λ is coefficient of frictional resistance, L is tunnel length (m), D is tunnel diameter (m), g is gravitational acceleration rate(m/s^2), A_m is projected area of vehicles (m^2), n_t is number of vehicles in tunnel, n_{jf} is number of jet fans in operation, K_j is coefficient of pressure rise by jet fans, A_j and is discharge area of jet fans (m^2).

A branch consists of the beginning node, *i* and the end node, *j*. And the total pressure loss in the branch (h_L) can be interpreted as the difference in the total airflow energy between two nodes. All the forces including the frictional pressure loss are balanced as the Bernoulli's equations shown in Equations (5) to (6): Equation (5) in the unit of pressure (in *Pa*, *SI* unit) and Equation (6) in the unit of head (most commonly in *mmAq*).

$$p_i + \frac{\rho}{2}v_i^2 + \rho g z_i = = p_j + \frac{\rho}{2}v_j^2 + \rho g z_j + \rho g h_L \quad (5)$$

$$\frac{p_i}{\gamma} + \frac{v_i^2}{2g} + z_i = \frac{p_j}{\gamma} + \frac{v_j^2}{2g} + z_j + h_L \quad (6)$$

The first term in Equation (5) and (6) represents static pressure, while the second and third terms stand for dynamic pressure and potential pressure, respectively. Without any shock loss involved, the fourth term shows the pressure loss due to friction. The relationship between airflow rate and pressure loss in a branch can be defined by the power model as in Equation (7); the pressure loss is proportional to the nth power of airflow rate. *K* is dimensionless resistance factor. *K* is correlated to Darcy's friction coefficient (λ) as shown in Equation (8).

$$h_L = KQ^n \quad (7)$$

$$K = \lambda\frac{L}{D}\frac{1}{2g{A_r}^2} \quad (8)$$

The continuity equation describing the mass conservation at a node is defined in Equation (9), while Equation (10) shows that the energy

balancing condition in the network theory requires that the sum of the pressure losses in all branches contained in a closed mesh should be zero.

$$\sum_{l\epsilon S_{in}} \rho Q_l - \sum_{l\epsilon S_{out}} \rho Q_l + \rho q_l = 0 \quad (9)$$

$$H_i - H_j = \sum_{l\epsilon lmesh} h_{L,l} = \sum_{l\epsilon lbranch} K_l |Q_l|^n = 0 \quad (10)$$

S_{in} and S_{out} imply inflow and outflow branches, respectively; Q and q are the unknown airflow rate and the addition of airflow at nodes. H is the enthalpy, that is, the total energy at each node. In addition, $lmesh$ are a set of branches associated with a single mesh.

The total pressure related to a branch including friction loss (h_L) and shock loss (sh_L) can be expressed as in Equation (11).

$$\begin{aligned} h_L + sh_L + \Delta P_m - \Delta P_t - \Delta P_{jf} &= \left(K + K_2 - \frac{b}{A_r}\right) Q^2 \\ &+ \left(\frac{2bV_t + c}{A_r}\right) Q \\ &+ \left(aV_n^2 - bV_t^2 - cV_j\right) \end{aligned} \quad (11)$$

K and K_2 are the dimensionless coefficients of pressure loss due to friction and shock, respectively.

2.1. Hardy – Cross method

The most commonly used analytical technique of the network-type tunnels is Hard-Cross method. This method first defines the fundamental meshes and guesses the initial values for the airflow rate ($Q_l^{(0)}$) in each branch which satisfy the mass conservation law as shown in Equation (9). Pressure loss in individual branches with the initial flow rate is calculated by Equation (7) and then the results are evaluated to see whether the conditions in Equation (10) are met in each fundamental mesh. If Equation (10) is not met, then all the values for the airflow rate in each branch must be adjusted. A same incremental value of the airflow rate (ΔQ_{mesh}) in each mesh can be calculated using Equation (12) proposed by Hardy Cross (Cross, H., 1936).

$$\Delta Q_{mesh} = -\frac{\sum_{l\epsilon mesh} K_l Q_l^n}{\sum_{l\epsilon mesh} nK_l |Q_l|^{n-1}} = -\frac{\sum_{l\epsilon mesh} K_l Q_l^n}{\sum_{l\epsilon lmesh} n \left|\frac{h_{L,l}}{Q_l}\right|} \quad (12)$$

The incremental value of the quantity of flow in each mesh is repeatedly calculated by Equation (12). In each iteration, the new values for the airflow rate are adjusted by Equation (13) which implies that the new airflow rate for each branch can be obtained by adding all the incremental values ($\Delta Q_l^{(m)}$) to the values ($\Delta Q_l^{(m-1)}$) in the previous iteration. This iteration continues until the increment values for all fundamental meshes become less than the given tolerance. The final airflow rates for all the branches are found by Equation (13).

$$Q_l^{(m)} = Q_l^{(m-1)} \pm \sum_{l\epsilon mesh(l)} \Delta Q_{lmesh} \quad (13)$$

The subscript *mesh(l)* means a set of meshes that contain the branch *'l'*.

The Hardy-Cross method seems to be a very straightforward algorithm to apply. However, Equation (12) could have a problem of convergence associated with the algorithm to select fundamental meshes of large scale networks because it includes truncation errors by Talyer theorem. And it is reported to need to adjust relaxation factors to improve convergence (Dubin, Ch., 1947, Williams, G. N., 1973).

2.2. A new algorithm for the tunnel ventilation network solution

Let's assume the incidence matrix that shows the relationship between branches and source nodes is A_{10}, *[NB x NS]* matrix. The incidence matrix defining the relationship between branches and non-source nodes is assumed to be *A12, [NB x (NN-NS)]* matrix, while that between branches and meshes is *A13, [NB x NM]* matrix. Theses matrices are defined as in Equation (14) to (16).

$$A_{10}(i,j) = \begin{cases} +1 & \text{if branch } i \text{ ends at node } j \\ -1 & \text{if branch } i \text{ starts at node } j \\ 0 & \text{Otherwise} \end{cases} \quad (14)$$

$$\begin{cases} +1 & \text{if branch } i \text{ ends at node } j \end{cases}$$

$$A_{12}(i,j)=\begin{cases}-1 & \text{if branch } i \text{ starts at node } j\\ 0 & \text{Otherwise}\end{cases} \quad (15)$$

$$A_{13}(i,j)=\begin{cases}+1 & \text{if flow in branch } i \text{ is in the same direction as mesh } j\\ -1 & \text{if flow in branch } i \text{ is in the opposite direction as mesh } j\\ 0 & \text{if branch } i \text{ is not in mesh } j\end{cases} \quad (16)$$

NB, NN, NS and *NM* are the number of branches, nodes, source nodes and meshes, respectively, while *NN-NS* becomes the number of start nodes. And A_{01}, A_{21}, A_{31} are the transposed matrices of A_{10}, A_{12}, and A_{13}, respectively. The continuity equation at each node defined in Equation (9) can be expressed as $A_{21}Q = q$, while the energy equations in branches and meshes can be written as $h = A_{12}$ and $A_{31}h = 0$, respectively. Since the pressure loss in a branch is defined as $h_{ij} = K_{ij}Q_{ij}^{n}$, it can be expressed by the matrix form as shown in Equation (17). A_{11} in Equation (18) can be rearranged as a diagonal matrix of *[NB x NB]*.

$$h = A_{11}Q^{n} \quad (17)$$

$$A_{11} = diag(K_l|Q_l|^{n-1}); \mathrm{l} = 1, 2, \ldots.\mathrm{NB} \quad (18)$$

As the ventilation force in branches can be expressed by a squared term of the quantity of flow, the total pressure loss in the branches can be expressed by a quadratic function of the quantity of flow as shown in Equation (19). And the pressure loss associated with the unknown quantity of flow *(Q)* can be expressed by the general equation as shown in Equation (20) according to the Newton-Raphson method.

$$h(Q) = A.Q^{2} + B.Q + C \quad (19)$$

$$h(Q) = h(q) + h'(q).(Q - q) = = D.Q + D' \quad (20)$$

$$D = 2A.q + B = 2\left(K + K_2 - \frac{b}{A_r}\right).q + \left(\frac{2bV_t + C}{A_r}\right) \quad (21)$$

$$\mathrm{D}' = \mathrm{C} - \mathrm{A}.q^{2} = \left(aV_n^{2} - \mathrm{b}V_t^{2} - cV_j\right) - \left(K + K_2 - \frac{b}{A_r}\right).q^{2} \quad (22)$$

Where *A, B, C, D* and *D'* are replacement constants, *Q* is the unknown flow rate in the next stage of iteration ($Q^{(m)}$), and q is the flow rate in the previous iteration stage ($Q^{(m-1)}$).

Due to the difficulties in selecting the fundamental meshes, Hamam and Brameller (1972) and Todini and Pilati(1987) suggested the method that can simultaneously solve the quantity of flow in branches (Q) and pressure of nodes (H). This method called the branch method or sometimes the gradient method does not require mesh selection and the network is composed with the only branch and node information. While the size of matrix must be large enough to contain all the branches and nodes, its advantages are relatively short computation time and better convergence.

Todini and Pilati (1987) presented the following equation by using the energy conservation equation in branches and the mass conservation equation in nodes as shown in Equation (23 (See Equation (14) to (18)).

$$\begin{bmatrix}A_{11}A_{12}\\ A_{21}0\end{bmatrix}\begin{bmatrix}Q\\ H\end{bmatrix} = \begin{bmatrix}-A_{10}H_0\\ q\end{bmatrix} \quad (23)$$

Where, H_0 matrix of *[NS x 1]* represents the source nodes that respond to A_{10} as in Equation (14).

However, since Equation (23) cannot be solved directly due to the non-linear terms, the unknowns for the flow quantity and pressure can be derived through iteration. Equation (24) to (26) can be obtained from Equation (23) to apply schemes of Newton - Ranpson types.

$$\begin{bmatrix}nA_{11}^{*}A_{12}\\ A_{21}0\end{bmatrix}\begin{bmatrix}\Delta Q\\ \Delta H\end{bmatrix} = \begin{bmatrix}dE\\ dq\end{bmatrix} \quad (24)$$

$$dE = A_{11}Q^{(m)} + A_{12}H^{(m)} + A_{10}H_0 \quad (25)$$

$$dq = A_{21}Q^{(m)} - q \quad (26)$$

Where, the right hand side of the equation, (*dE, dq*) contains the residual values in the mth iteration. *dE* is the unbalanced residual of the pressure loss by the flow increment in branches (ΔQ) and the pressure increment (ΔH) in nodes, while *dq* is the unbalanced residual of the flow quantity in nodes by the flow increment (ΔQ) in branches. In general, $A_{11}^{*}$is identical to A_{11}. But if there is a constant term like '*C*' in Equation (19), it becomes$A_{11} - (C/Q)$; that is $A_{11}^{*} = A_{11} - diag(C/Q)$.

The flow and pressure increments, ΔQ and ΔH in Equation (24), can be rearranged as shown in Equation (27) to (29).

$$\begin{bmatrix}\Delta Q\\ \Delta H\end{bmatrix} = \begin{bmatrix}nA_{11}^{*}A_{12}\\ A_{21}\ 0\end{bmatrix}^{-1}.\begin{bmatrix}dE\\ dq\end{bmatrix} = \begin{bmatrix}B_{11}B_{12}\\ B_{21}B_{22}\end{bmatrix}.\begin{bmatrix}dE\\ dq\end{bmatrix} \quad (27)$$

$$\Delta Q^{m} = B_{11}.dE + B_{12}.dq = Q^{(m-1)} - Q^{(m)} \quad (28)$$

$$\Delta H^{(m)} = B_{21}.dE + B_{22}.dq = H^{(m-1)} - H^{(m)} \quad (29)$$

Solving Equations (28) and (29) directly after replacing nA_{11}^{*} with G, Equations (30) and (31) can be obtained and Equation (31) can be expressed as shown in Equation (32) (Ayres, F., 1974).

$$Q^{m} = (I - G^{-1}.A_{11})Q^{(m-1)} - G^{-1}\left(A_{12}H^{(m)} + A_{10}H_{0}\right) \quad (30)$$

$$H^{(m)} = -[A_{21}G^{-1}A_{12}]^{-1}\{A_{21}G^{-1}\left(A_{11}Q^{(m-1)} + +A_{10}H_{0}\right) - \left(A_{21}Q^{(m-1)} - q\right)\} \quad (31)$$

$$\alpha H^{(m)} = \beta \quad (32)$$

Where, it's $\alpha = [A_{21}G^{-1}A_{12}]$ and $\beta = -\{A_{21}G^{-1}\left(A_{11}Q^{(m-1)} + A_{10}H_{0}\right) - (A_{21}Q^{(m-1)} - q)\}$.

As Equation (32) is a function of the flow quantity ($Q^{(m-1)}$) in the iteration *(m-1)th* iteration, the flow quantity in the current m^{th} the iteration ($Q^{(m)}$) can be calculated directly by deriving the pressure value ($H^{(m)}$) in the m^{th} iteration and then substituting it in Equation (30).

3. Development of a network model

3.1. Overview

Table 1. List of tunnel ventilation programs.

Program	Tunnel	GUI	Network method		Remark
NETVEN	Road	×	○	Hardy-cross (Incomp.)	Korea (1997)
TVSDM	Road	×	×	- (Incomp.)	Korea (1999)
TUNVEN	Road	×	×	- (Incomp.)	USA (1979)
IDA RTV	Road	○	○	? (Incomp.)	Sweden (1995)
S.E.S	Subway	×	○	MOC (Incomp.)	USA (1997)
VentSim	Mine	○	○	Hardy-cross (Incomp.)	UK (1994)
ThermoTun	High-Rail	×	×	MOC (Comp.)	UK Online

To list a few, Table 1 shows the programs developed for road, subway and railroad tunnels and mine airways. As a lot of time and expenses for analyzing 3D CFD are required despite the latest computer technology development, extensive numerical analyses are often difficult to carry out. However, owing to the recent CPU and memory technology development, one-dimensional programs for analyzing the ventilation and air pressure in the road, subway and express railroad tunnels can be integrated. IDA RTV/Tunnel program from Sweden provides the models that can analyze the ventilation as well as the disaster prevention in road, subway (Station), and express railroad tunnels by offering GUI environment. Even though the program does not have the model for analyzing the compressible air pressure, it is expected that this model can be integrated without any difficulty. The analysis of the programs listed in Table indicates that development of a comprehensive tunnel ventilation model is desirable and the model should include capability to provide the GUI environment and analyze the compressibility and incompressibility-based network-type tunnels.

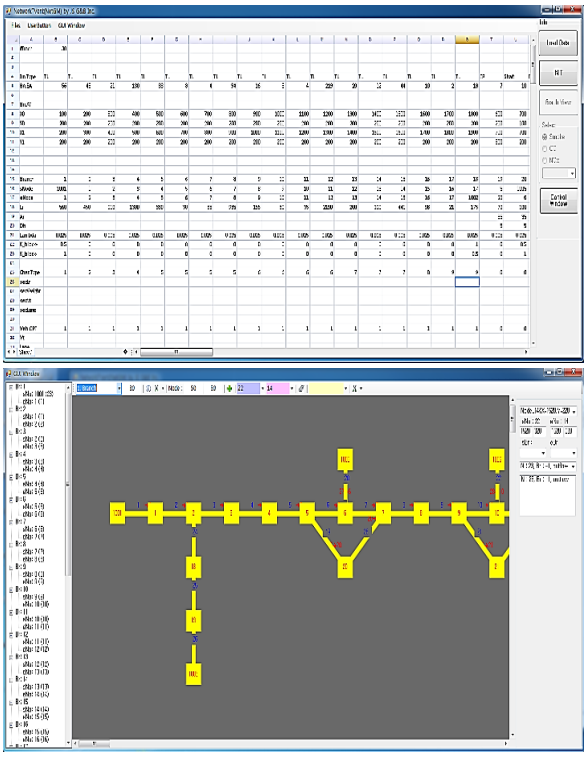

Figure 1 Newly developed network model (NetworkTVent).

In this study, a program that can analyze air quantity and pollutant concentration in the network-type tunnels was developed based on the theories described above. The new method that can minimize the limitations of Hardy-Cross algorithm was applied to the program. Visual Basic.NET was used as a development language. And for the input data, ReoGrid was used to make users enter data in a form of excel sheets by considering the network's complexity. And GUI was separately developed (See Figure 1.).

3.2. Method for calculating the airflow rate and the pollutant concentration

As aforementioned, the logical flow to determine the airflow rate in network-type tunnels is summarized in Figure 2. The Gradient method is used as the analytical solution algorithm. This method has the advantages over Hardy Cross algorithm since it can simultaneously solve pressure and the airflow rate without composing the fundamental meshes in the complicate network.

Figure 3 shows the concept for estimating the pollutant concentration in tunnel. The entire length a tunnel can be divided into a number of equal length branches and the pollutant concentration in each branch can be calculated by the concept in Figure 3 after the airflow rate is determined by the aforementioned algorithm. The pollutants transport is assumed to be one dimensional and be governed only by advection. And the airflow rate and the pollutant concentration within equal length branch is assumed to be uniform.

Considering advection and turbulent diffusion mechanisms at the same time, the one-dimensional pollutant transport equation can be expressed as in Equation (33). Excluding the turbulent diffusion, the equation can be reduced to Equation (34) which is applied to TUNVEN model (Lee, 1997a, Ryu, 1999).

$$\frac{\partial C}{\partial t} + \frac{\partial}{\partial x}(UC) = D\frac{\partial^2 C}{\partial x^2} + \frac{C_i q_i}{A} - \frac{C q_0}{A} + S_v + \tilde{R} \qquad (33)$$

In which:

C: Pollutants concentration (ppm).

C_i: Pollutants concentration in the inflow (ppm).

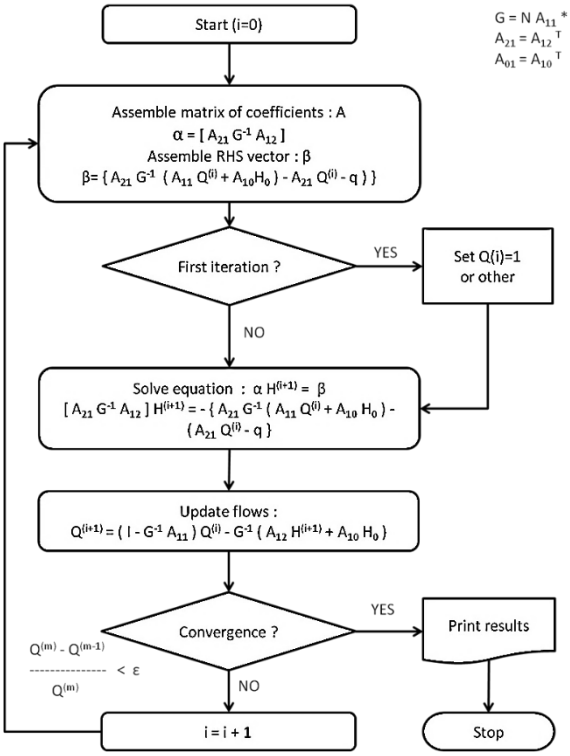

Figure 2. Flowchart of main steps in gradient method.

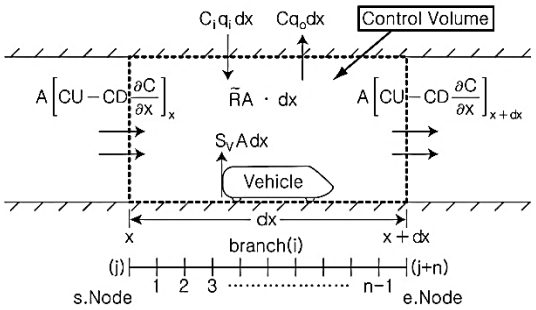

Figure 3. Mass balance for pollutant in tunnel element control volume.

U: Air velocity in tunnel (m/s).

A: Cross section of tunnel (m^2).

D: Diffusion coefficient (Total diffusivity, m^2/s).

S_v: Generation of pollutants by vehicles (ppm/s).

$\tilde{R}$: Generation of pollutants by chemical reactions (ppm/s).

q_i, q_o: Airflow rate of inflow and outflow per unit length ($m^3/(s.m)$).

$$U\frac{\partial C}{\partial x} = \frac{C_{q_i} - C_{q_0}}{A} + S_v \qquad (34)$$

Lee et al. (1997b) and Kolon Co. Ltd. (1998) reported that if there are unidirectional air

movements, the effect of turbulent diffusion is relatively low compared to advection. So concentration prediction only by the advective diffusion is enough. Turbulent diffusion can play an important role in the situation with the ultra-low air velocity created by bi-directional traffic in tunnels. And the turbulent diffusion is prominent near the portals showing significantly high gradient of concentration. In general, the transport of pollutants in tunnels is governed mostly by the advection, while the turbulent diffusion is limited with the diffusion coefficient of 0.18-0.50 m^2/s (Sato et al., 1985). The ratio of advection to the total transport is defined as Péclet (Pe) number (=$U.L/D$) and Ryu (1999) showed that in contrast to the molecular diffusion in the air, the number is in the range of 10^3 to 10^4 in the tunnels less than 1km. And in the numerical algorithm the terms of second-order derivatives can be ignored.

Therefore, only advective diffusion is assumed as the only transport mechanism, while the transport between adjacent equal-length branches can be handled by the the finite difference method. Change in the air velocity between inlet and outlet of a branch can be defined by difference between the rates of inflow and outflow. So when the airflow rate in the i^{th} branch is defined by $(U.A)_i$, the concentrations at j^{th} node and $^{(j+1)th}$ node of the branch can be defined by Equation (35).

$$C_{j+1} = C_j + \left(1 - \frac{(\Delta Q_0)_i}{(U.A)_i}\right) + C_{amb} \cdot \frac{(\Delta Q_i)_i}{(U.A)_i} + \frac{\left(\Delta Q_{req} \cdot Q_{Limit}\right)_i}{(U.A)_i} \quad (35)$$

Where:

C_j, C_{j+1}: Concentrations at jth node and $(j+1)^{th}$ node of the i^{th} branch (1/m or ppm)

C_{amb}: Ambient concentration in the inflow into the i^{th} branch

$(U.A)_i$: Airflow rate in the i^{th} branch (m^3/s)

$(\Delta Q_i)_i$, $(\Delta Q_0)_i$: Airflow rates added to and extracted from the i^{th} branch (m^3/s)

$\left(\Delta Q_{req}\right)_i$, $(Q_{Limit})_i$: Required ventilation rate (m^3/s) and permissible limit (1/m or ppm) in the i^{th} branch

Equation (35) is applicable to the case that the air in the i^{th} branch flows from j^{th} to $(j+1)$ node. The RHS first term shows effects of the airflow rate removed through ducts, while the second term is related to the inflow added through ducts. The air supplied to the i^{th} branch through ducts is assumed to be the ambient air. The third term represents the concentration increase due to the pollutant emission from vehicles.

The first term can have a negative value if the airflow rate extracted through ducts is larger than the flow rate within the i^{th} branch. Therefore, the branch length has to be properly adjusted to avoid negative figures. The length should be small not to include excessive number of ducts, and Equation (36) is recommended as the criterion to optimize the number of branches.

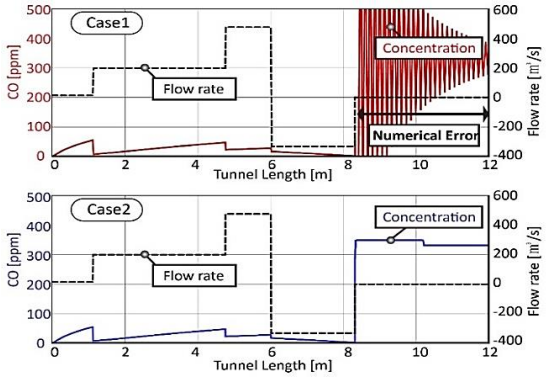

Figure 4. Numerical error by the number of sub-branch.

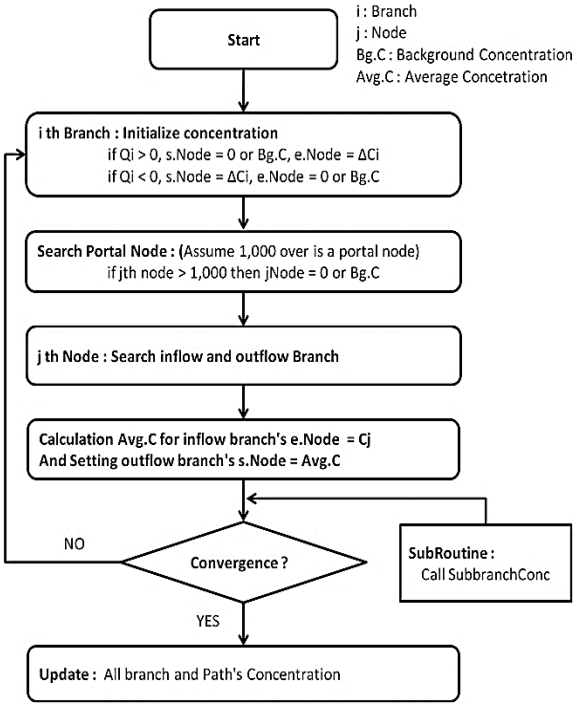

Figure 5. Flowchart of concentration calculation.

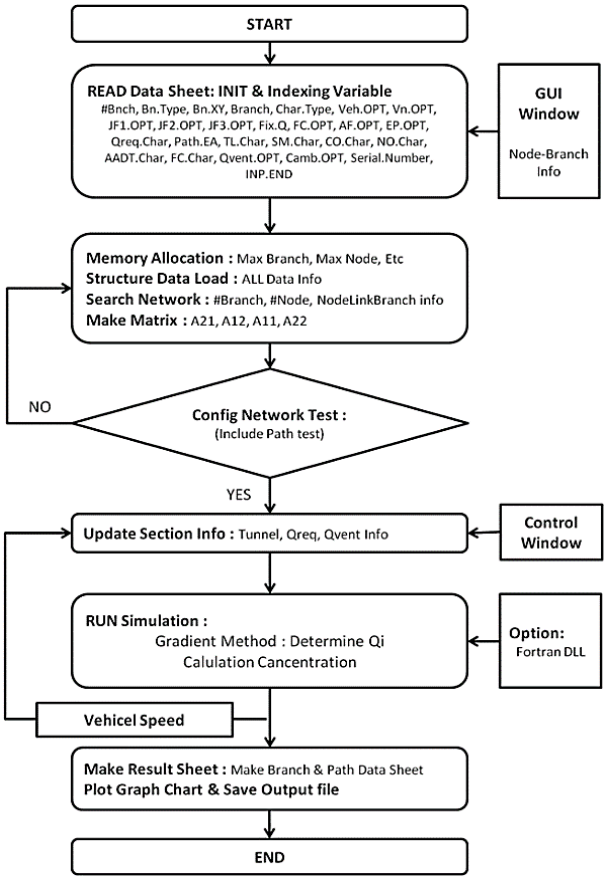

Figure 6. Flowchart of network model.

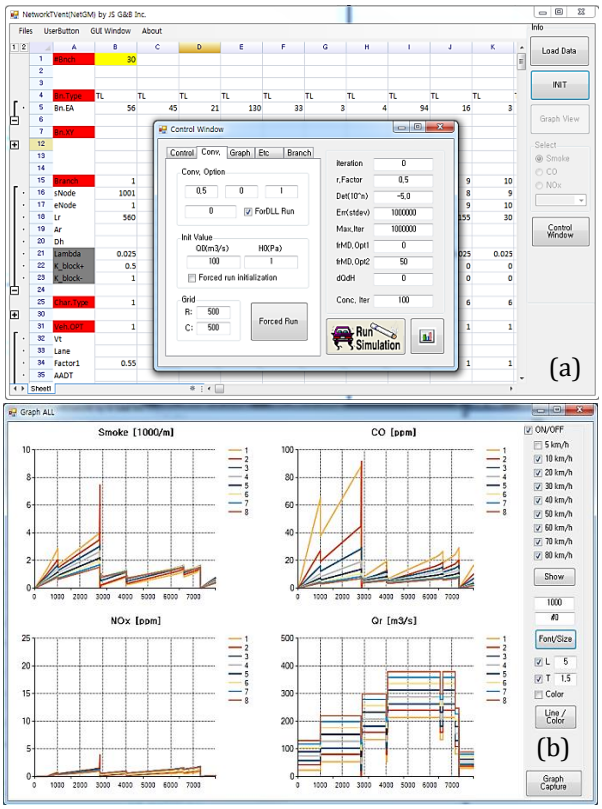

Figure 7. Network model(Running example). (a) Main Window and Control Window; (b) Plot concentration and ventilation flow rate.

$$n_i = int[(\Delta Q_0)_i/(U.A)_i + 0.5] \quad (36)$$

Figure 4 represents analytical cases about the transverse systems with supply and exhaust ducts. Case 1 shows a numerical error due to the insufficient number of branches, while Case 2 describes results of the analytical analysis of the concentration profile with proper number of branches.

The analytical steps to calculate the concentrations in network-type tunnels are summarized as follows, and Figure 5 shows the flow chart.

Step 1. Assume the initial concentration values in all branches

(Concentration values at the start and end nodes; start and end nodes are determined according to the flow direction in branches)

Step 2. Identify the nodes connected to the atmosphere and use the ambient concentration as the initial values at those nodes (p. Node = 0 or ambient concentration).

Step 3. Identify the inflow and outflow branches connected to each node (Set Inflow = + *n* branch and outflow = -*n* branch)

Step 4. Calculate the weighted average concentration at the end node of the inflow branch for all branches.

Step 5. Then use the value at the end node as the initial values at the start node of the branch connected. If there is outflow branch connect, then use the concentration vale in the branch as the initial value at the start node of the outflow branch.

Step 6. Repeat Step 3 through 5 until the concentration conditions are satisfied (Go back to Step 2 when the conditions are not satisfied.)

Step 7. Update the results in all branches or in all paths

The above procedure for concentration determination is illustrated as a flow chart shown in Figure 6 and the realized program is shown in Figure 5, while Figure 6 shows the flow chart for the whole program. Figure 7 are the screenshots taken during the data input and after the execution.

3.3. Comparison of calculation times

Table 2. Comparison of the program execution times.

Computer			Case 1	Case 2
CPU (RAM)	CPU Clock	Fortran DLL	Branch: 30EA SubGrid: 967EA r.factor: 0.5	Branch: 30EA SubGrid: 967EA r.factor: 0.1
32Bit (4GB)	2.67 GHz	×	309 sec	1,466 sec
		○	178 sec	794 sec
64Bit (8GB)	2.50 GHz	×	182 sec	866 sec
		○	106 sec	483 sec

Table 2 summarizes calculation times required for program execution under the convergence criterion of 10^{-5}. One 32-bit and one 64-bit desktop computers with Window 7 were used to test improvement of calculation times. In the table, effects by the number of bits is greater than those of CPU Clock. Reduction of the calculation time by computer bits, application of Fortran DLL for inverse matrix calculation and adjustment of the relaxation factor was 39-41%, 41-45% and 77-79%, respectively. Therefore, it can be concluded that application of the optimal relaxation factor results in faster convergence compared to the specifications of computer itself.

4. Applications of the network model

4.1. Case of a single-tube connected with slip tunnels

In order to analyze the ventilation of the complex network-type tunnels, a tunnel shown in Figure 8 connected with two entry tunnels and one exit tunnel was studied. The physical and ventilation characteristics of the Case 1 tunnel are listed in Table 3 and its network structure is illustrated in Figure 8 (Lee, et al, 1997b).

Table 3. Physical characteristics and ventilation system of Case 1.

Branch		1	2	3	4	5	6	7
Physical characteristics	Length [m]	785	500	275	205	75	320	215
	Cross-section Area [m²]	85.4	106.3	85.4	85.4	42.1	52.8	52.8
	Hydraulic Dia. [m]	Estimated $D_h = 4.763 \times 10^{(-2)} \times A_r + 5.138$						
	Darcy friction factor	0.019	0.018	0.019	0.017	0.021	0.020	0.020
	Shock loss factor	inlet : 0.5, outlet : 1.0, junction : 0.0 ~ 1.0						
	Wind [m/s]	-	-	-	6.5	-	6.5	-
Traffic data (HGV=11%)	Speed [km/h]	23	23	18	60	23	60	18
	Traffic rate [veh/hr]	4190	5566	3862	5118	1376	1704	1256
	Lane [lane(s)]	3	4	3	3	1	1	1
Ventilation system (Jet fan)	J/F dia. [mm]	1270	1270	-	1270	-	630	630
	No [ea]	1	1	-	2	-	2	2
	Efficiency [%]	90	90	-	87	-	90	90

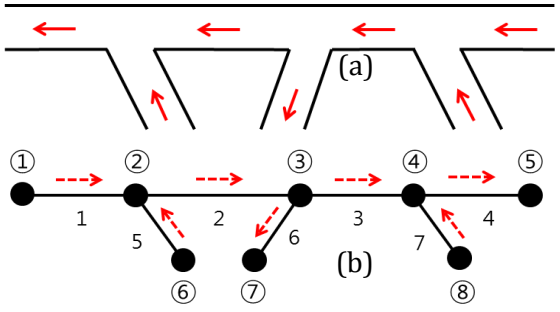

Figure 8. Complex network tunnel (Case 1). (a) tunnel type; (b) network structure.

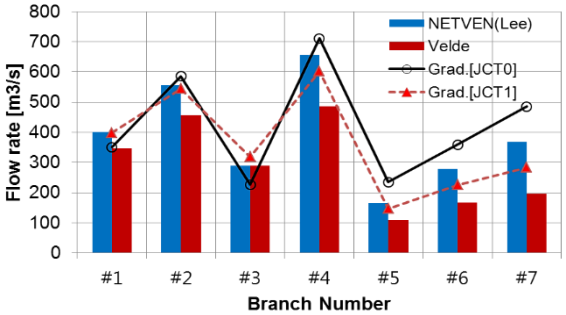

Figure 9. Comparison of estimated ventilation rates (Case 1).

Figure 9 shows the results and comparisons are made along with the works by Velde (1988) and (Lee, et al, 1997b). Compared with the output by Velde (1988), the airflow rates in slip tunnels calculated by the non Hardy-Cross algorithm are higher. The discrepancies might be created due to ignorance of the atmospheric wind direction particularly acting on Branches 4 and 6 by Velde. In addition, shock loss factors in the junctions and drag coefficients were also not taken into account by Velde. The results from non Hardy-Cross algorithm application is very close to the output from NETVEN model (Lee, et al, 1997b); it is the case regardless of consideration of the shock loss at the junctions. The discrepancies are mainly due to the differences in shock loss coefficients at the entrance and exit portals and junctions, and application of the hydraulic diameter in non Hardy-Cross algorithm model.

4.2. Case of a two-tube tunnel connected with slip tunnel

In order to analyze the airflow rate in the case of a twin tunnel with the fixed-quantity branches (Q_{Fix}), a 1.5km-long twin tunnel with evacuation passageway and two slip tunnels in each direction was analyzed. As shown in Figure 10, the two-lane twin tunnels with the cross-sectional area of 63.62 m² have 3 evacuation passageways (A=19.64 m², L = 50 m) (Branch 17, 18, and 19) at 250m intervals and 4 inclined slip tunnels (Branch 13, 14, 15, 16). The vehicle speed and the traffic volume were 60 km/hr and 4,000 veh/hr, respectively. Four jet fans (Φ1250 mm) were installed near the entrance portal in each tunnel (Branch 1, 7). The natural ventilation of 2.5 m/s was applied to the main tunnel (Branch 1 to 6 and 7 to 12) in the opposite direction to the traffic flow (See Figure 10).

Table 4 shows the scenarios for Case 2 to 5; Case 2 only with the piston effects created by the vehicle traffic, Case 3 with the piston effects plus the fan operation, Operation of the fan in an evacuation passageway (Branch 18) further added to Case 4 and two fans in the passageways (Branch 17, 19) even further added to Case 5. When the four fans were turned on, the air velocity induced into each tunnel in operation increases from 4.43 m/s to 8.48 m/s. The airflow rates through the two passageways (Branch 17,

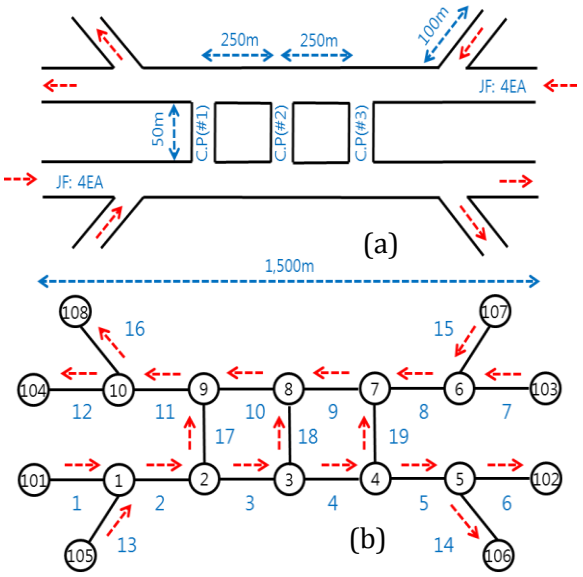

Figure10. Complex network tunnel (Case 2~5). (a) tunnel type; (b) network (node and

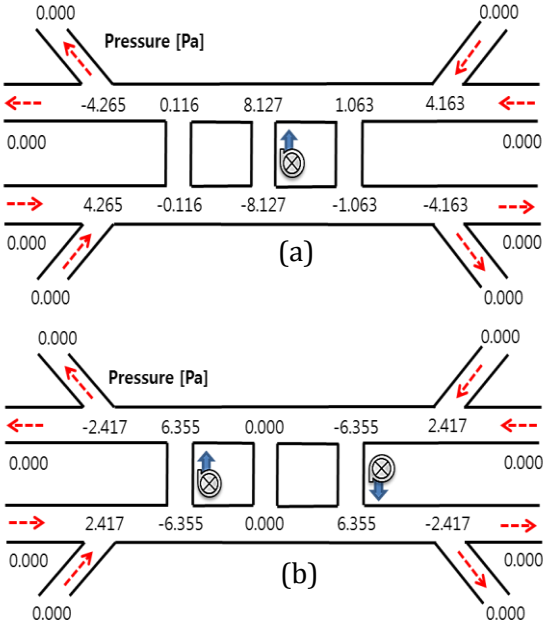

Figure11. Pressure profiles for Case 4-5. (a) Case 4 (#1: off , #2: 100 m³/s, #3: off); (b) Case 5 (#1: 100 m³/s, #2: off, #3: -100 m³/s).

19) are identical, while the middle passageway (Branch 18) shows no airflow. Without fan operation as in Case 2, the airflow rate through the entrance portal is equal to that in the exit portal, while operation of 8 fans in the main tunnels results in reversed airflow through the entering slip tunnel near the entrance portal and increased airflow rate through the entrance portal

(4.43→8.48 m/s) and the exit portal (4.43→5.16 m/s) and also through the exit slip tunnel (5.81→6.65 m/s) close to the exit portal.

In Case 4, a fan was turned on to secure the fixed airflow rate of 100 m^3/s in the middle evacuation passageway (Branch 18) in the direction described in Figure 10. The total airflow rate induced to the main tunnel through the entrance portal (10.27 m^3/s) and the entering slip tunnel is a little bit larger than the airflow rate (10.14 m^3/s) leaving the tunnel through the exit portal and exiting slip tunnel. The airflow distribution in two tunnels are symmetrical since only the fan in the middle passageway was switched on. However, the pressure profiles shown in Figure 11 indicates that the pressure is negative in most part of the lower tunnel since the fan was turned on in the direction from the lower to the upper tunnel.

In Case 5, two fans in the first and third passageways (Branch 17, 19) were on in directions opposite to each other with the fixed airflow rate of 100 m3/s. Operation of the two fans secures the required airflow rate through the passageways as well as the symmetrical airflow distributions. The results show that the airflow rates are symmetrical between the upper and lower tunnel and also symmetrical between the first and second halves of the tunnel. In all scenarios, the door in the passageway was always kept open.

Table 4. Velocity profiles for Cases 2-5.

Case	Jet fan	Q_{Fix} (m^3/s)	Velocity profiles [m/s]
2	OFF	OFF	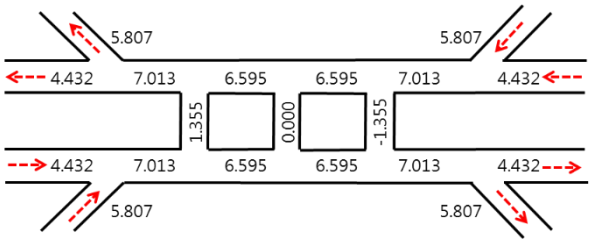
3	ON (φ1250; x 4EA)	OFF	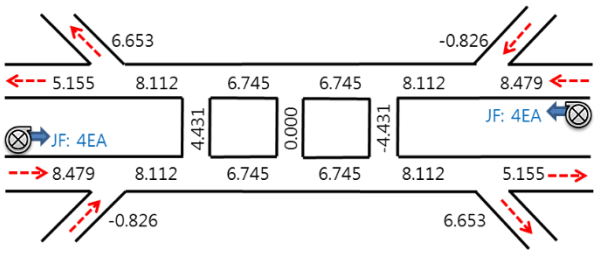
4	OFF	ON (#1: 0; #2: 100; #3: 0)	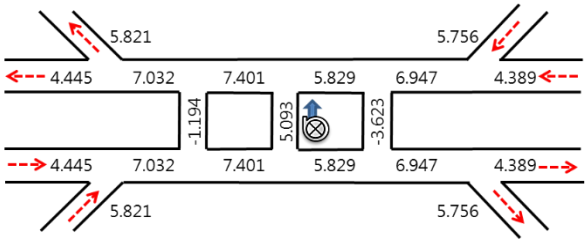
5	OFF	ON (#1: 100; #2: 0; #3: -100)	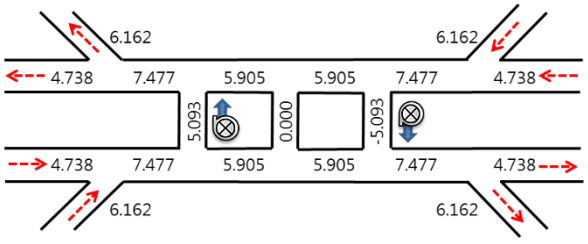

4.3. Verification of the air velocity in single-tube tunnels

Table 5. Input data (Case 6).

Type	Values
Tunnel length	3,000 m
Cross section area	75.862 m2
Hydraulic diameter	8.776 m
Vehicles	185.1 veh/tunnel (Am = 2.997m2)
Qreq (Smoke)	630.2 m3/s (at 60 km/h)
Natural wind speed	Vn = -2.5- 0 m/s

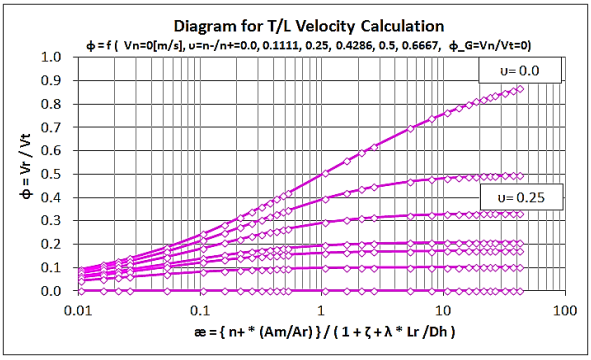

Figure 12 Diagram for tunnel air velocity calculation(D. Stokic).

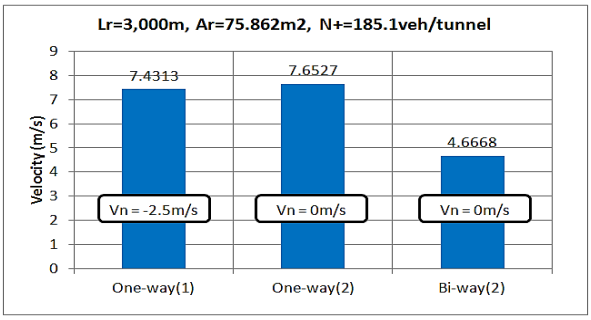

Figure13. Calculation results by the network model (Case 6).

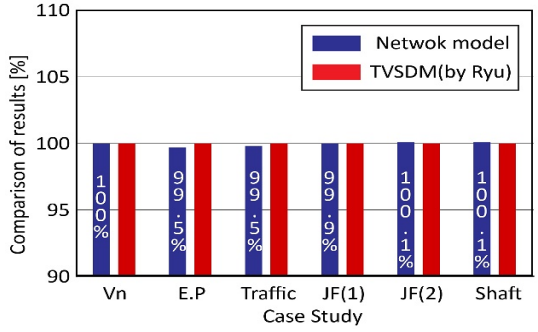

Figure 14 Comparison of the average velocity between Network model and TVSDM (Case 7-12).

(Stokic, 1976) reported the distribution of the air velocity in tunnels created only by the traffic flow and without the natural ventilation ($V_n=0$). He used the dimensionless variables (Φ, æ) and showed the results as in Figure 12. *æ* along the x axis denotes the dimensionless variable representing the traffic volume and the tunnel characteristics, while Φ along the y axis is the ratio of the air velocity in tunnel to the vehicle velocity. Therefore, the airflow rate in tunnel can be obtained directly from the Stokic's line diagram in Figure 12 using the traffic and tunnel characteristics.

For the single-tube tunnel, to evaluate the applicability of the analytical model enveloped in this paper, a single-tube 2-lane tunnel with the length of 3,000 m was analyzed. The cases for uni-directional and bi-directional traffic were the targets for the analysis. The main in-out parameters for the analysis of Case 6 is summarized in Table 5. The analysis results are shown in Figure 13. The number (1) in Figure 13 implies the situation where the natural wind of 2.5 m/s is induced against the traffic flow, while the number (2) is the case without the natural wind. The air velocities in the cases of uni-directional and bi-directional traffic can be derived by Stokic's line diagram as follows:

- In case of uni-directional traffic tunnels ($v=0$, $v_n=0$),

$$\text{It is } æ = \frac{185.1.\left(\frac{2.9971}{75.862}\right)}{1+0.6+0.025.\left(\frac{3,000}{8.776}\right)} = 0.721;$$

$$\Phi = \frac{1}{1+(0.721)^{-0.5}} = 0.459$$

So the air velocity is found to be $V_r = 0.457.60/3.6 = 7.65$ m/s.

- In case of bi-directional traffic tunnels ($v=0.25$, $v_n=0$), Φ is 0.28 in the diagram. So the air velocity is found to be $V_r = 0.280.60/3.6 = 4.67$ m/s.

Comparing the results from the non Hardy-Cross algorithm model and Stokic's line diagram, they are found to match very well. Cases 7-12 were the scenarios with different conditions for the natural wind, the piston effects, the jet fans, the electric precipitators and the ventilation shafts, respectively. in a 2,000m-long tunnel with AADT of 29,492 veh/day, HGV of 0%, and cross-sectional of 39.82 m^2. Figure 14 shows the comparisons with TVSDM (Ryu, 1999) program

with respect to the air velocity. The air velocities derived from the network model studied in this paper is very similar to those found with TVSDM showing the relative differences less than 1%.

4.4. Analysis of the urban tunnels exclusively for small vehicles

Analysis of the air velocity and the pollutant concentration in network-type urban tunnels exclusively for small vehicles was carried out in a network-type tunnel shown in Table 6 and Figure 15. The required airflow rate in terms of CO was assumed to be 25 m3/s per Km to predict the CO concentration in tunnel. The ventilation rate of 25 m3/s per Km is generally required rate in urban tunnels exclusively for small vehicles in Korea.

Case 13 in Figure 15 is the twin-tube tunnel where the two tubes are completely separated due to the closed doors in Branch 13, 15, 16, and 17. On the contrary, in Case 14, the air flow between the two tubes is possible with open doors in those branches.

Table 6. Input data for the complex network tunnel (Case 13-14).

(a) Branch data						
Branch	L_r (m)	A_r (m^2)	Shock loss factor	Vn (m/s)	J.Fan Φ1030	EP (m^3/s)
1,7	500	50.61	0.5	-2.5	5	
2,8	500	50.61		-2.5		
3,9	2,000	50.61		-2.5		
4,10	850	50.61		-2.5		
5,11	50	50.61		-2.5		
6,12	100	50.61	1	-2.5		
13,15,16,18	30	20				
14,17	30	20				80
19,21	50	20				
20,22	50	20				80

(b) Traffic data			
Vehicle type (%)		Vehicle frontal area	
Passenger car	83.0	Small vehicle	2.31 m2
Small bus	7.0		
Heavy bus	0	Large vehicle	7.11 m2
Small truck	10.0		
Medium truck	0	Number of lane	
Heavy truck	0	2	

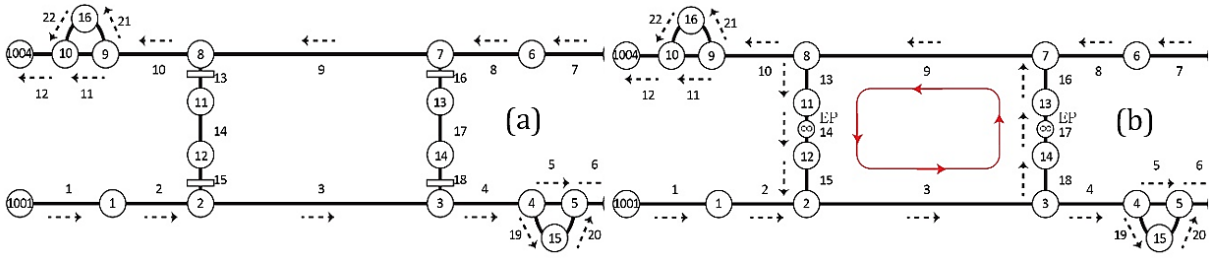

Figure15. Complex network tunnel. (a) Case 13 (branch 13, 15, 16, 17: closed); (b) Case 14 (branch 13, 15, 16, 17: open).

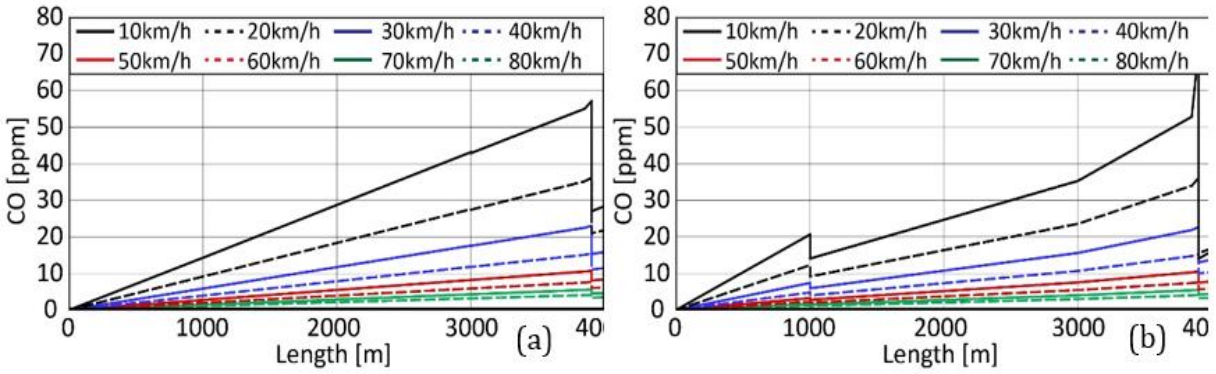

Figure16. CO concentration profiles. (a) Case 13; (b) Case 14.

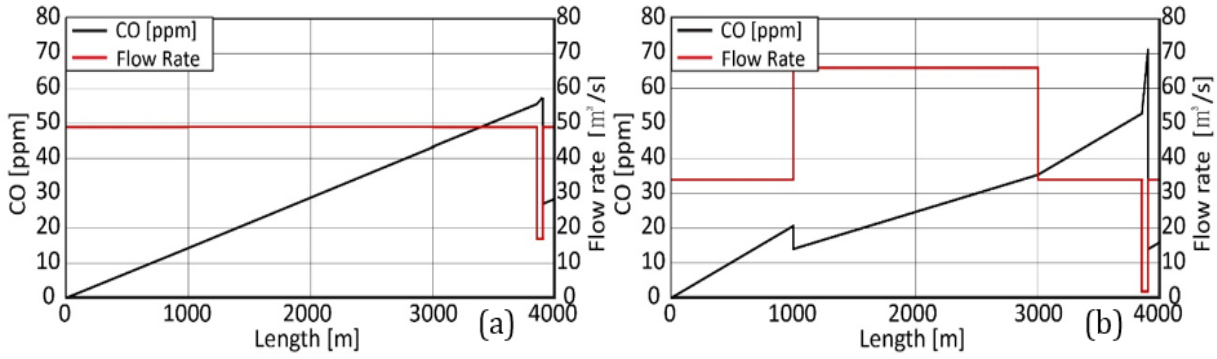

Figure17. Flow rate and CO concentration at the vehicle speed of 10km/h. (a) Case 13; (b) Case 14

This is the case where dust scrubbers and gas purifiers are installed in so-called by-pass branches and the cleaned air from one tube is allowed to be recirculated to the other tube through the passageway between them. Figure 15 shows two electric precipitators are installed in Branch 14 and 17.

Figure 16 is the graphs showing CO concentration profiles along the lower tube in Figure 15. The results clearly show that Case 14 with recirculation strategy led to relatively lower concentration than Case 13 where recirculation is not allowed.

Examining Figure 17 plots the airflow rate and the CO concentration distributions in the tunnel at the vehicle speed of 10 km/h. Even though installation of the electric precipitators can reduce the CO concentration inside the tunnel, Case 14 allowing recirculation shows the CO concentration within the branches close to the entrance portal such as Branch 1, 2 and 7, 8 is higher than Case 13 without recirculation. This is due to the reduced piston effects and also jet fan pressure; the reason is mainly due to the increased airflow rate in the middle part of the tunnel. Therefore, the ventilation method employed in Case 14 can create imbalance of the airflow rate over the entire length of the main tubes and this limitation is likely to generate less piston effects and lower fan pressure rise. Consequently this may make it even more difficult to control the distribution of airflow rate in the network-type tunnels with various types of slip tunnels. Therefore, whether the recirculation ventilation strategy should be allowed or not depends on the pollutant emission reduction requirement, budget for equipment installation, recirculation, that is, reuse of the air, and automatic control necessity.

5. Conclusions

Recent development in Korea and overseas shows that in congested urban area, network-type tunnels become more common. This trend implies that the current tunnel ventilation criteria mainly designed for the single-tube tunnel must be reviewed again. This paper analyzed the theoretical limitations involved in the local and overseas models for the vehicle tunnel ventilation system design and proposed a new concept of the

algorithm "non Hardy-Cross iteration algorithm" to solve the airflow rate distribution in complex network-type tunnels. In addition, a new program is de developed for analyzing the airflow rate and the pollutant concentration in network-type tunnels. The major contents of this study can be summarized as follows:

1. Due to the widely-known limitations of Hardy-Cross algorithm, development of a more efficient method to analyze the tunnel ventilation network based on the non Hardy-Cross method was the main goal of this study.

2. The new analytical logic of non Hardy-Cross algorithm developed in this study is Gradient method. The branch (often called as gradient) method was applied to analyze the airflow rate and the pressure without composing the fundamental meshes. In addition, a method for defining relatively short branches was studied to treat the divergence problems due to the extremely low flow rate in the transverse ventilation system where supply and exhaust ports are located at short intervals.

3. The calculation efficiency was found to be improved by adjusting the relaxation factor rather than the computer specifications such as Bit or RAM. Selecting a proper relaxation factor in the analytical program developed in this study reduced the calculation time by 77 to 79%.

4. Comparisons with the existing models were made. Based on the analysis results in a single-tube tunnel, accurate comparison was difficult with Velde's model due to lack of detailed information about the natural ventilation force and the vehicle drag coefficient in Velde's model. Comparisons with Lee's model are found to match very well. However, in case of twin-tube tunnels with slip tunnels, operation of fans in evacuation passageway led to the symmetrical distribution of the airflow rate and the pressure between two tubes and also between the first and second halves. These are the typical characteristics found in the existing models employing the Hardy-Cross algorithm.

5. In the comparative study with Stokic's line diagram and TVSDM, the air velocity derived by the gradient method matches well with differences less than 1%. And the ventilation system with bypasses equipped with electric precipitators installed near the exit portal was found to be less efficient than the system installed at the center. However, installing the bypass at the center leads to reduction of the airflow rate induced through the entrance portal due to the decreased piston effects and fan pressure rise. Careful control measures are required to deal with the situation showing unbalanced airflow rate profiles.

6. Since more network-type tunnels are expected to be constructed in urban areas, the current tunnel ventilation system design standards focused mainly on the single-tube tunnels should be reviewed again. This requirement is even more necessary for the network-type tunnels with entering and exiting slip tunnels to optimize the ventilation and control systems.

6. Acknowledgment

This research was supported by a grant project 17SCIP-B066321-05 (Development of key subsea tunneling technology) from the Infrastructure and Transportation Technology Promotion Research Program funded by the Ministry of Land, Infrastructure and Transport of the Korean government.

References

Ayres, F., 1974. Matricses, Schau's outline series, McGrawHill Book Co, pp. 1-100.

Ayres, F., 1974. "Matricses", Schau's outline series, McGrawHill Book Co, pp. 1-100.

Choi, J. H., 2016. Construction of urban underground road: attractive alternative for reducing traffic congestion, *Ksce journal of civil engineering*, Vol. 64, No. 8, pp 33-37.

Cross, H., 1936. Analysis of flow in networks of conduits or conductors. University of illinois, engineering experimental station, *Bulletin* No. 286, pp.62-97.

Dubin, Ch., 1947. Le calcul des reseaux mailles. contribution al' application pratique de la methode hardy cross la houille blanchem mai-juin, pp. 213-223.

Hamam, Y. M., Brameller, A., 1971. Hybrid Method for the Solution of Piping Networks. *Proceedings institution of electrical engineers*, Vol. 118, No. 11, pp.115-132.

Kolon CO. Ltd., 1998. Development of the Optimal Design System for the Vehicle Tunnel Ventilation System. KEC-97-C10-2, pp. 1-174.

Lee et al., 1997a. Development of a simulation model for the vehicle tunnel ventilation using network theories. *Proceedings of the 1st asian rock mechanics symposium*.

Lee et al., 1997b. Simulation Modeling of the vehicle tunnel ventilation system using network theory. *KSGE*, Vol. 34, pp. 617-629.

Ryu et al., 1999. Study on the desing technique of the road tunnel ventilation system. SAREK, 1999 *Proceedings of the summer symposium*, 99-S-054, pp. 329-336.

Stokic, D., 1976. Diagram for tunnel air velocity calculation due to simultaneous action of traffic and outer meteorological influences. 2nd AVVT, 1976, D3-45 D3-56

Todini, E., Pilati, S., 1987. A gradient algorithm for the analysis of pipe networks. *Proceedings international conference on computer applications for water supply and distribution*, Leicester polytechnic, 8-10 September, pp.45-82.

Velde, K., 1988. A computer simulation for longitudinal ventilation of a road tunnel with incoming and outgoing slip roads. *Proceedings of the 6th international symposium on the aerodynamics and ventilation of vehicle tunnels*, Durham, UK, p. C3-179 ~ C3-201.

Williams, G. N., 1973. Enhancements of Convergence of Pipe Network Solutions. *J. of the hydraulics division, ASCE*, Vol. 99, No. HY7, pp. 1057-1067.